Fourier Transform Infrared (FTIR) Study and Thermal Decomposition Kinetics of Sorghum bicolour *Glume and* Albizia pedicellaris *Residues*

Ayokunle O. Balogun, Olumuyiwa A. Lasode, Hui Li & Armando G. McDonald

Waste and Biomass Valorization

ISSN 1877-2641
Volume 6
Number 1

Waste Biomass Valor (2015) 6:109-116
DOI 10.1007/s12649-014-9318-3

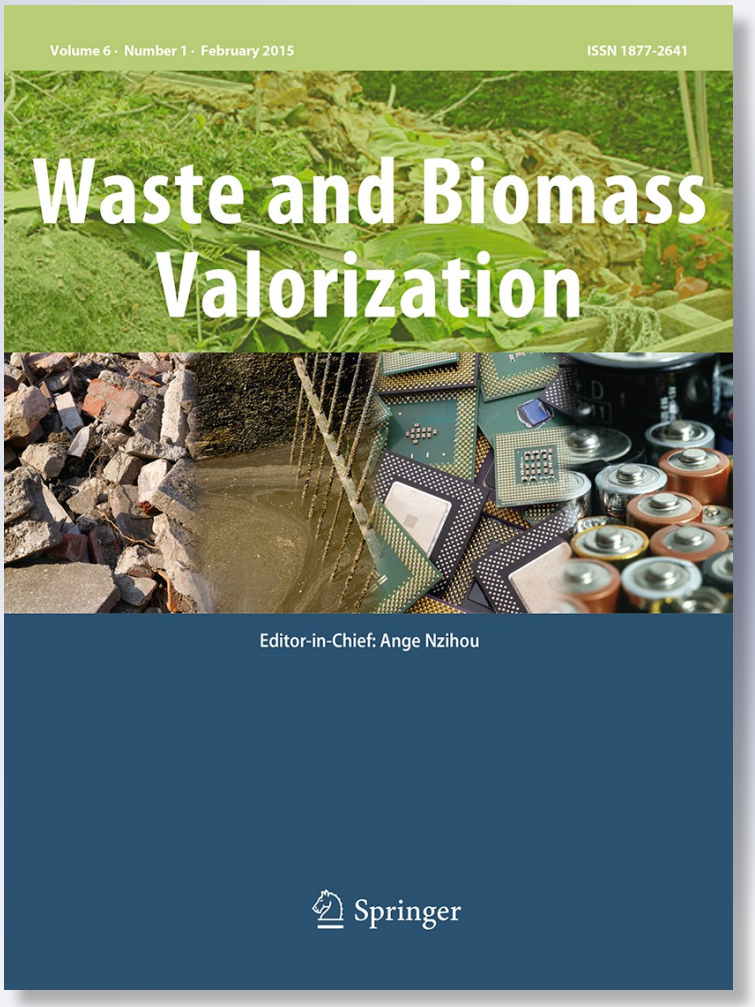

Springer

Waste Biomass Valor (2015) 6:109–116
DOI 10.1007/s12649-014-9318-3

ORIGINAL PAPER

Fourier Transform Infrared (FTIR) Study and Thermal Decomposition Kinetics of *Sorghum bicolour* Glume and *Albizia pedicellaris* Residues

Ayokunle O. Balogun · Olumuyiwa A. Lasode · Hui Li · Armando G. McDonald

Received: 26 March 2014 / Accepted: 14 July 2014 / Published online: 22 July 2014

Abstract An investigation into the thermal decomposition kinetics, by thermogravimetric analysis, of an agricultural and a forestry residue was carried out using distributed activation energy model (DAEM) and Friedman's differential technique. Preliminarily, Fourier transform infrared spectroscopy alongside proximate, ultimate and heating value was used in the characterisation of the biomass resources. The characterisation experiment showed differences between *Sorghum bicolour* glume (SBG) and *Albizia pedicellaris* (AP). The activation energy (E) showed a significant variation as conversion progresses; recording E using DAEM for AP (169–291 kJ mol^{-1}) and for SBG (212–283 kJ mol^{-1}), while E (Friedman's model) for AP (188–314 kJ mol^{-1}) and SBG (163–280 kJ mol^{-1}). The correlation coefficients obtained for both models (DAEM; $R^2 \geq 0.976$, Friedman; $R^2 \geq 0.971$) were high; attesting to the suitability of the models. The reaction order n was also evaluated as a function of temperature based on Avrami's theory. The average values (0.209 and 0.195) of n obtained for AP and SBG, respectively were found to be lower than those from literature. This places emphasis on the probable effect of biomass complex structure on the reaction order in biomass thermochemical conversion process.

A. O. Balogun · H. Li · A. G. McDonald
Department of Forest, Rangeland and Fire Science, University of Idaho, Moscow, ID 83844-1132, USA

A. O. Balogun · O. A. Lasode (✉)
Department of Mechanical Engineering, Faculty of Engineering and Technology, University of Ilorin, P.M.B. 1515, Ilorin, Nigeria
e-mail: oalasode@yahoo.com

Keywords DAEM · Friedman's technique · Reaction order · Biomass · Decomposition kinetics

Introduction

Biomass is an attractive alternative energy source that possesses immense renewable potentials. It is noted for diverse and widespread availability at an inexpensive price and its utilisation has no net effect on the global carbon cycle, if used in a sustainable manner [1]. *Sorghum bicolour* glume (SBG) and *Albizia pedicellaris* (AP) are biomass species from agricultural and forestry residues respectively that are found in abundance in Nigeria. For instance, an FAO data estimated that 11.37×10^6 t of *S. bicolour* residue is generated, while 7×10^6 m^3 of wood wastes residue are reported to be produced annually from logging and sizing operations [2, 3]. Thus, lignocellulosic biomass is potentially capable of tackling the dwindling fossil fuels reserves, the environmental concerns provoked by greenhouse gas (GHG) emissions and assist in broadening the narrow energy supply spectrum plaguing the country.

The use of lignocellulosic resources as feedstock for bioenergy purposes is usually preceded by characterisation because these resources are composed of numerous species with different chemical character and they differ significantly from one biomass to the other. Proximate, ultimate and the heating value determination have been applied for biomass characterisation extensively and these give insight into the basic difference among the various biomass classifications [4]. In addition, infrared spectroscopy is a powerful technique that is sensitive to structural features and has been valuable in biomass characterisation [5, 6]. For instance, it can give information on the degree of crystallinity of the

polysaccharide components and the structural features of biomass [6–8]. Therefore, in this study, Fourier transform infrared (FTIR) spectroscopy in conjunction with the basic characterisation methods has been employed for biomass characterisation.

The application of biomass for energy generation or chemical extraction mostly requires the deployment of thermochemical conversion techniques. The reaction rate is a crucial parameter in the conversion processes because it differs distinctly as a function of temperature, heating rate and pressure [5]. Moreover, the lack of homogeneity in the composition of lignocellulosic resources also initiates intricate decomposition reactions with varying rates; thus, making investigation into biomass kinetics a fundamental research goal. Decomposition kinetics is essential for the prediction of reaction behaviour, the optimisation and control of thermal degradation processes and the efficient design of thermal reactors [9]. There exists several models for the determination of biomass degradation kinetics; however, the distributed activation energy model (DAEM) is remarkable.

After DAEM was initially conceived by Vand [10], its application was largely confined to the analysis of coal pyrolysis and thermal regeneration reaction of activated carbon [11, 12]. Lately, however, DAEM has been employed in the evaluation of reaction kinetics of biomass thermal decomposition processes [13, 14]. Unlike conventional models that are derived for the analysis of a single reaction, DAEM is predicated on the assumption of a couple of irreversible first order parallel reactions with different rate coefficients occurring simultaneously [15]. It incorporates a normalised distribution curve function; Gaussian distribution is commonly adopted, which represents the different activation energies of the proposed reactions. The need for an assumption of constant activation energy is obviated and being a parallel reaction model, conversion-dependent activation energy determination is easier to incorporate than in other mathematical models [16].

Traditionally, the activation energy, the frequency factor and the reaction model are the objects of interest in kinetic modelling, while the reaction order is mostly assumed. Lately, the convention of adopting first order of reaction indiscriminately is being challenged as models with n^{th} order of reaction have shown to be more accurate in most cases [17, 18]. From the foregoing, the primary objective of this study was to investigate the reaction kinetics of biomass decomposition under non-isothermal thermogravimetry using DAEM as well as the Friedman's differential technique for comparison. The reaction order will also be evaluated at several temperature levels. The authors are not aware of any literature on the application of DAEM for the determination of the kinetic parameters and FTIR study of SBG and AP biomass resource.

Experimental

Samples Preparation

SBG was sourced from a farm site (8°37′N, 4°46′E) in the city of Ilorin, Nigeria in December 2012. The maturity period of the *S. bicolour* plant is about 6 months. After harvesting, the panicles were threshed and the glumes handpicked. The SBG were air dried in the laboratory for about 1 month. AP (from 40 to 45 year old trees) was sourced from a timber processing plant (8° 27′N, 4°35′E) in the city of Ilorin in December 2012, chipped (about $15 \times 10 \times 10$ mm^3), and air-dried. The two biomass samples were milled (Thomas Wiley mill model 4, 1 mm screen) to a particle size between 0.25–1.00 mm.

Characterisation and Thermogravimetric Analysis (TGA)

The biomass samples were subjected to proximate, elemental and TG analyses according to international standards as detailed by Balogun et al. [19]. The TGA measurements were run on multiple heating rates of 5, 10 and 15 K min^{-1} on a Perkin Elmer TGA-7 instrument. The original vacuum dried biomass was analysed by FTIR spectroscopy using an Avatar 370 spectrometer (ThermoNicolet) in the single bounce attenuated total reflection (ATR) mode (SmartPerformer, ZnSe). Two spectra were gathered in the scan region of 400–4000 cm^{-1} with a resolution of 4 cm^{-1} and an accumulation of 64 scans. An average spectrum was generated and subsequently ATR and baseline corrected mathematically with the OMNIC v7 software [20].

Higher Heating Value (HHV) Determination

The HHV was evaluated using the correlation equations developed by Friedl et al. [21]. Equations (1) and (2) are based on ordinary lest squares (OLS) and partial least squares (PLS) regressions respectively, which were derived from the test of 122 different biomass materials.

$$HHV(OLS) = 1.87C^2 - 144C - 2802H + 63.8CH + 129N + 20147 \quad (1)$$

$$HHV(PLS) = 5.22C^2 - 319C - 1647H + 38.6CH + 133N + 21028 \quad (2)$$

where C is carbon, H is hydrogen and N is nitrogen contents expressed on dry mass percentage basis. The HHV was reported as an average of the two equations.

Kinetic Study

Distributed Activation Energy Model (DAEM)

Distributed activation energy model has been applied extensively in the determination of kinetic parameters of biomass decomposition [22]. It assumes a complex reaction of numerous irreversible, first-order parallel reactions occurring all at the same time. Each reaction possesses a characteristic rate parameter [15]. The model expresses change in total volatile, V, with respect to time, t, as:

$$1 - \frac{V}{V^{\varepsilon}} = \int_0^{\infty} \Phi(E,T) f(E) dE \tag{3}$$

$$\Phi(E,T) = exp\left(-\frac{A}{\beta} \int_{T_0}^{T} e^{-\frac{E}{RT}} dT \right) \tag{4}$$

where, V is volatile mass loss (%), V^{ε} is volatile content (%) and $f(E)$ is the distribution function of the activation energy. Combining Eqs (3) and (4), and following a series of simplification steps through approximations [15], DAEM is expressed as:

$$\ln \frac{\beta}{T^2} = \ln \frac{AR}{E} + 0.6075 - \frac{E}{RT} \tag{5}$$

A linear relationship is established between the plot of $\ln(\beta/T^2)$ and $1/T$ with β as heating rate (K min^{-1}), T as temperature (K), A as frequency factor (min^{-1}), R as universal gas constant (8.314 J mol^{-1} K^{-1}) and E as activation energy (J mol^{-1}).

Friedman Method

The global kinetic rate equation is written as:

$$\frac{d\alpha}{dt} = Aexp^{\left(-\frac{E}{RT}\right)} f(\alpha) \tag{6}$$

It has been argued that at constant degree of conversion, the reaction rate is only a function of temperature [23].

$$\frac{d\ln(d\alpha/dt)_{\alpha}}{dT^{-1}} = -\frac{E_{\alpha}}{R} \tag{7}$$

The rearrangement and integration of Eq. (7) gives rises to Eq. (8) popularly attributed to Friedman [24].

$$\ln\left(\frac{d\alpha}{dt}\right)_{\alpha} = constant - \frac{E}{RT} \tag{8}$$

where α denotes degree of conversion. A plot of conversion rate against the inverse of temperature will result in a linear relationship from which E can be deduced.

The reaction order is another important variable in the determination of biomass kinetics aside the activation energy. In this study, the reaction order will be calculated according to the expression of Avrami's theory [25].

$$\alpha = 1 - \exp\frac{-k(T)}{\beta^n} \tag{9}$$

where α, $k(T)$, and β are the same variables defined in Eqs. (5) and (8), and n is the reaction order. Taking double logarithm and transposing, Eq. (9) may be exprsed as

$$\ln(-\ln(1-\alpha)) = lnA - \frac{E}{RT} - nln\beta \tag{10}$$

For a given temperature, T, the plot of $\ln(-\ln(1-\alpha))$. Against $ln\beta$at different heating rates gives a linear relationship and the reaction order n can be deduced from the slope of the graph.

Results and Discussion

Proximate and Ultimate Analyses, and HHV Determination

Biomass characterisation is a necessary preliminary step to most bio-based applications either for energy generation or chemical extraction. It gives a basic understanding of the energy capabilities, physical and chemical characteristics of the prospective feedstock. Table 1 presents the result for the proximate, ultimate analyses and the HHV determination for the biomass residues. The result had been extensively discussed in a previous publication [19].

FTIR Spectroscopy of Biomass Residues

The lignocellulosic cell wall comprises of a supermacromolecular complex of hemicellulose, cellulose and lignin fractions and the composition varies with the biomass resource. FTIR spectroscopy has been used as a tool to examine the chemical composition and functional groups of biomass. Figure 1 shows the spectra, while Table 2 presents the spectral band assignment of AP and SBG. The bands at 2,914 cm^{-1} (SBG) and 2,924 cm^{-1} (AP) are indicative of C–H stretching from aliphatic structure of extractives and polymer, while the absorption peaks (C=O ester stretch) in the region of 1,720–1,740 cm^{-1} may be attributed to the presence of acetyl group in hemicellulose compounds and/or the bond between hemicellulose and lignin [6, 7, 26].

The bands at about 1,604 and 1,510 cm^{-1}, which are assigned to aromatic skeletal vibrations, are all characteristic bands of lignin [6, 27]. The bands at 1,422 cm^{-1} indicates the presence of a mixture of crystalline cellulose I

Table 1 Proximate and ultimate analyses, and heating values for biomass residues

Biomass	Proximate analysis[a] (wt%)			Elemental analysis[a] (wt %)				HHV (MJ kg^{-1})
	FC[b]	VM	Ash	C	H	N	O[b]	
AP	5.61±0.36	92.7±0.3	1.68±0.01	51.7±0.3	5.85± 0.38	0.54± 0.03	41.9±0.7	20.6±0.5
SBG	13.60±0.25	78.9±0.4	7.54±0.21	42.4±0.4	5.27±0.25	0.74±0.06	51.6±0.7	16.9±0.1

[a] Dry-basis, [b] calculated by difference

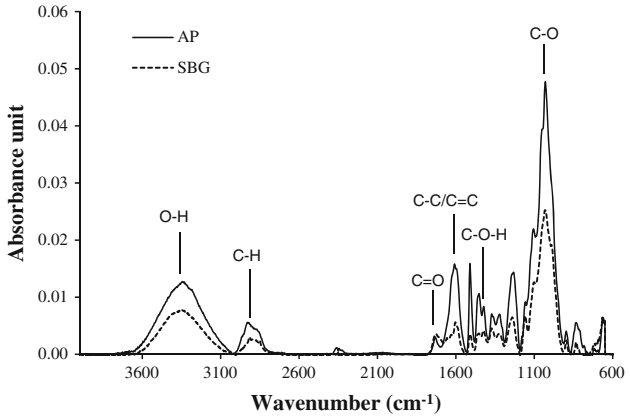

Fig. 1 FTIR spectra of AP and SBG biomass

Table 2 FTIR spectra band assignment for AP and SBG

Band assignment	Band (cm^{-1})		References
	AP	SBG	
O–H stretch	3,339	3,346	[6]
C–H stretch	2,924	2,914	[7], [27]
HC=O stretch (ester)	1,731	1,725	[6]
Aromatic C–C/C=C stretching modes	1,608, 1,510	1,604, 1,511	[6], [7]
$–CH_2$ scissor and aromatic ring vibrations	1,452	1,452	[6]
Aromatic ring vibrations and C–O–H in-plane bending	1,421	1,423	[6], [7]
O–H or C–H bending	1,371	1,371	[7]
C–O stretching	1,320	1,320	[6]
C–C and C–O stretch in guaiacyl	1,231	1,240	[6], [7]
C–O stretch H bonded system	1,157	1,158	[6]
C–OH stretch and C–H in-plane deformation in syringyl	1,105		[6]
C–OH and O–CH_3 stretch	1,030	1,031	[6], [7]
C–H wag	896	897	[6], [7]
C–H wag	833	833	[7]

and amorphous cellulose in AP and SBG [8]. The pronounced peak between 1,000 and 1,200 cm^{-1} is assigned to stretching vibrations from functional groups of hemicellulose and cellulose compounds [26]. An estimation of

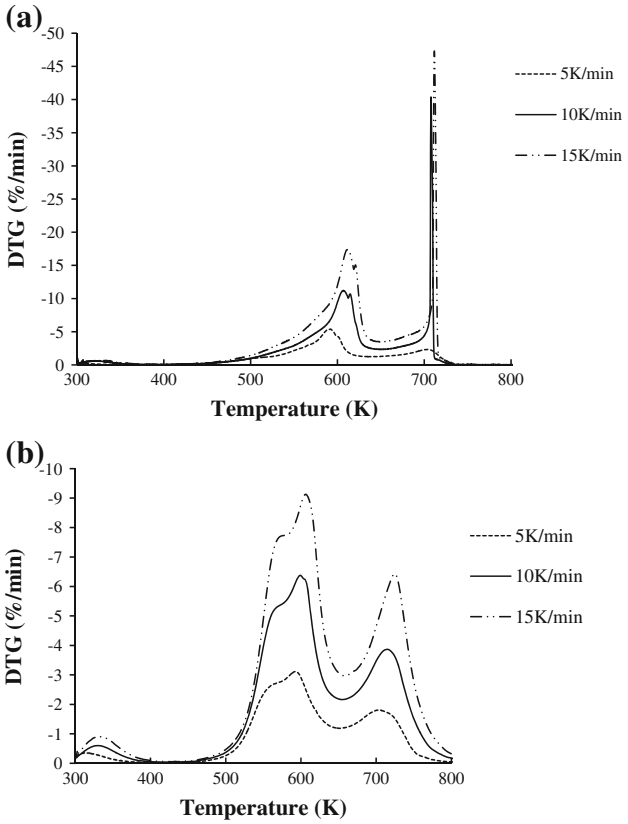

Fig. 2 Derivative TG (DTG) thermograms for **a** AP and **b** SBG at varied heating rates

cellulose crystallinity (CC) at the relative band height (H_{1429}/H_{897}) was used [28] and it was observed that the intensity ratio for SBG (0.75) was lower than for AP (1.1). This shows that SBG has a lower CC (and cellulose content) when compared to AP. The CC for AP, however, is comparable to the CC for hybrid poplar (1.6) [8], and chemical pulps (1.5–5.0) [28]. The reactivity of lignin is directly related to lignin syringyl to guaiacyl ratio (S/G) and the higher the S/G, the less condensed the lignin structure and therefore the easier it is to thermally degrade [29]. The relative band height (H_{1462}/H_{1510}) can be used to determine S/G by FTIR [30]. An estimated S/G ratio for AP (1.1) was lower than for SBG (4.8) but similar to hybrid poplar at 1.2 [31].

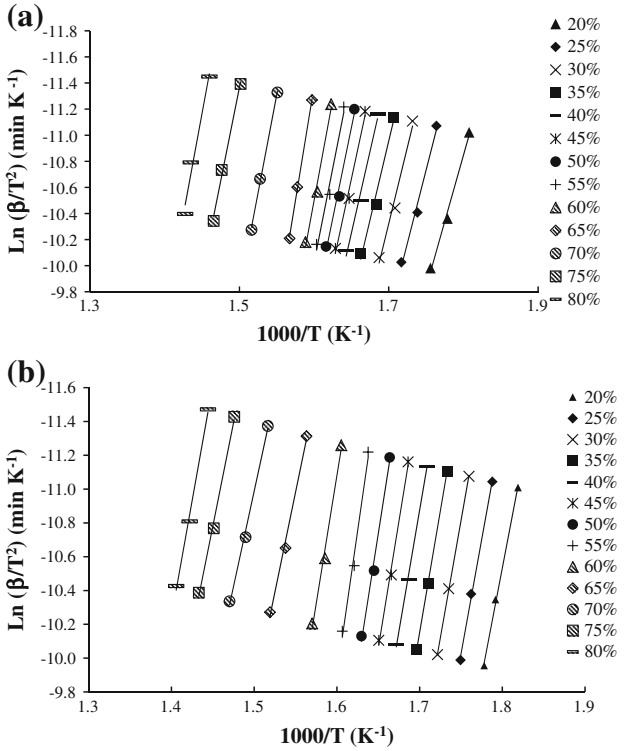

Fig. 3 A typical plot of isoconversional lines for the determination of E and A according to DAEM method at heating rates of 5, 10 and 15 K min^{-1} for **a** AP and **b** SBG

Biomass Degradation

Figure 2a and b shows the DTG thermograms for AP and SBG thermal degradation respectively at varied heating rates (5–15 K min^{-1}). A significant mass loss, which is indicative of moisture loss and probably degradation of light volatile organics, was observed below 400 K.

At about 500 K, the primary peaks started with characteristic shoulders that have been traditionally assigned to hemicellulose decomposition owing to its high reactivity [32]. The appearance of the first maxima DTG peaks around 586–610 K is indicative of cellulose decomposition [32, 33]. The influence of varied heating rates is illustrated by the thermograms as successive first maxima DTG peaks shift towards higher temperature with increasing heating rate. For instance, the DTG peaks for AP emerged at 586, 601, 607 K for 5, 10, 15 K min^{-1} respectively. The appearance of the secondary peaks above 700 K has been reported in literature and it has been adduced to the presence of some heavy chemical species in the biomass [19, 34, 35]. The last stage shows a gradual decomposition which has been attributed to lignin decomposition, lignin is considered to degrade over a wide temperature range [35].

Table 3 Activation energy (E) and correlation coefficients for conversion ratio of 0.20–0.80 for AP and SBG

α (−)	E DAEM (kJ mol^{-1})	A (min^{-1})	R^2	E Friedman's (kJ mol^{-1})	R^2
AP biomass					
0.20	168.58	2.52×10^{12}	0.993	188.17	0.998
0.25	186.09	2.73×10^{13}	0.989	199.86	0.979
0.30	194.83	8.39×10^{13}	0.984	205.62	0.982
0.35	201.26	1.71×10^{14}	0.983	218.89	0.988
0.40	208.90	4.90×10^{14}	0.984	229.20	0.990
0.45	221.14	3.88×10^{15}	0.987	240.56	0.984
0.50	231.78	2.27×10^{16}	0.985	252.81	0.980
0.55	240.83	9.40×10^{16}	0.981	265.68	0.983
0.60	257.18	1.45×10^{18}	0.988	280.61	1.000
0.65	291.47	5.04×10^{20}	0.999	313.94	0.971
0.70	249.89	3.42×10^{16}	0.998	225.57	0.997
0.75	237.61	7.50×10^{14}	0.993	243.17	0.985
0.80	257.30	7.34×10^{15}	0.976	243.17	0.985
Average	226.68			241.72	
SBG biomass					
0.20	212.23	3.34×10^{16}	0.998	225.42	1.000
0.25	225.93	2.96×10^{17}	0.998	231.58	1.000
0.30	230.27	3.41×10^{17}	1.000	228.78	1.000
0.35	238.44	9.10×10^{17}	1.000	236.54	0.997
0.40	238.43	4.40×10^{17}	0.999	240.84	0.992
0.45	249.47	2.22×10^{18}	0.995	254.92	0.989
0.50	259.67	8.90×10^{18}	0.992	274.55	0.980
0.55	283.39	4.52×10^{20}	0.988	280.30	0.990
0.60	250.87	2.35×10^{17}	0.992	194.11	0.995
0.65	196.86	1.91×10^{12}	0.995	163.37	0.993
0.70	187.59	1.04×10^{11}	0.996	184.92	0.996
0.75	203.29	6.92×10^{11}	0.996	222.97	0.996
0.80	227.47	2.28×10^{13}	0.995	258.31	0.996
Average	231.07			230.51	

Determination of Kinetic Parameters

The application of Eqs. (5) and (8) generates plots of isoconversional lines for AP and SBG and E was calculated from the slope of the graph at each conversion step. Figure 3 shows a typical plot of isoconversional lines obtained using the DAEM at heating rates of 5, 10 and 15 K min^{-1} for AP and SBG.

The calculation of the kinetic data was limited to the conversion ratio from 0.20 to 0.80 because outside this range there was little or no correlation. It has been noted that the early stage of biomass decomposition is essentially a physical process (dehydration), which cannot be adequately captured by chemical kinetic models [32]. Hence, its inclusion could introduce some error. The linear plots for both models showed an appreciably high correlation

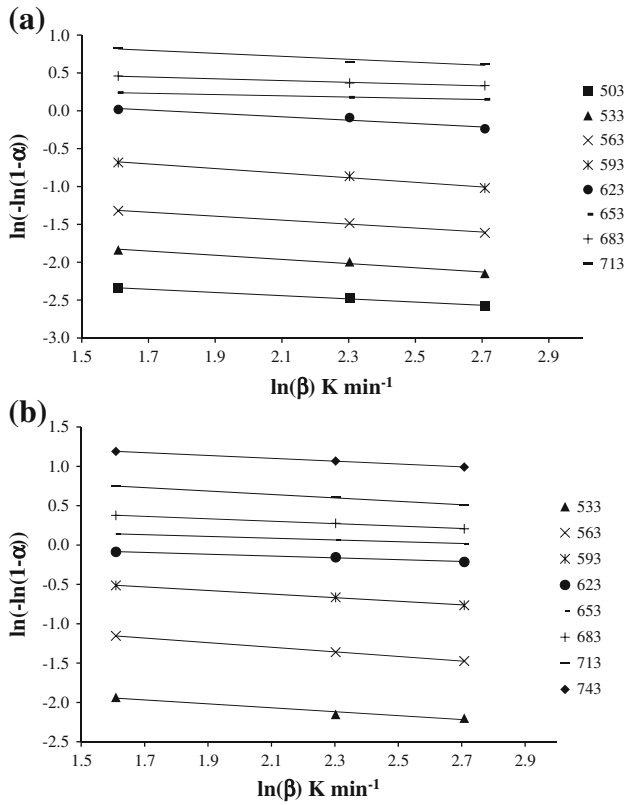

Fig. 4 Regression lines for the determination of reaction order according to Avrami's theory at 5, 10, 15 K min^{-1} for **a** AP and **b** SBG

coefficient ($R^2 \geq 0.976$; DAEM, $R^2 \geq 0.971$; Friedman) within the limits under consideration. This attests to the validity and the reliability of the models [5]. Table 3 shows that the values of *E* (DAEM) for AP ranges from 169 to 291 kJ mol^{-1} and for SBG from 212 to 283 kJ mol^{-1}, while the values of *E* (Friedman's) for AP ranges from 188 to 314 kJ mol^{-1} and SBG, from 163 to 280 kJ mol^{-1}. These values are in good agreement with those obtained in literature. For example, Chen et al. [32] and Kim et al. [33] reported that *E* for corn straw and pine tree, respectively ranged from 178 to 246 kJ mol^{-1} and from 145 to 302 kJ mol^{-1}. The values of *E* obtained from DAEM are generally lower than those from Friedman's technique for AP sample. However, both models return *E* values that rank close for SBG; yielding comparable average values of *E* (DAEM; 231 and Friedman's; 231 kJ mol^{-1}). Apparently, for either model *E* varies significantly as conversion progresses for the two samples; this is consistent with findings from literature regarding biomass kinetics [17, 32, 33]. The heterogeneous nature of lignocellulosic resources is largely responsible for this trend; consequently, pyrolysis kinetics of biomass residues is better explained as multi-step reaction mechanisms. It is noteworthy that after *E* reaches a peak at α of 0.65 and 0.55 for AP and SBG respectively, it deeps and rises again as conversion progresses. A similar observation was made in an earlier study on the devolatilisation kinetics of teak [36]. This trend is occasioned by the formation of new bonds arising from cross-linking, polycondensation or/and cyclisation reactions in char [37].

The *A* for AP was between 2.52×10^{12} and 5.05×10^{20} and SBG was 1.04×10^{11} and 4.52×10^{20} within the limits of the conversion ratio under consideration. A linear variation between *E* and *A* is observed; this is consistent with literature [36].

In the determination of kinetic parameters, an assumption on the reaction order is often made. However, the importance of reaction order in biomass decomposition kinetics has been aptly demonstrated in literature [18, 38]. For the investigation of biomass kinetics in this study, the dependence of the reaction order on temperature was evaluated at seven different temperature levels with multiple heating rates of 5, 10 and 15 K min^{-1}. The application of Avrami's theory in Eq. (10) generated the regression lines for AP and SBG as shown in Fig. 4, while the slope, the calculated values of *n*, and the R^2 are presented in Table 4.

The data in Table 4 show a high value of R^2 ($\geq$0.928); demonstrating the suitability of Avrami's method for the determination of *n* [17]. At 533–713 K, both samples exhibit similar variation with temperature. For instance, *n* for AP rises from 0.267 (533 K) to 0.303 (593 K), drops to 0.117 (683 K) and peaks at 0.197 (713 K), while for

Table 4 Slope, reaction order and correlation factor at temperature 533–713 K for AP and SBG

T (K)	Sample	Slope	n	R^2	Sample	Slope	n	R^2
533	AP	−0.276	0.276	0.979	SBG	−0.249	0.249	0.962
563		−0.261	0.261	0.993		−0.292	0.292	0.999
593		−0.303	0.303	0.989		−0.228	0.228	0.999
623		−0.223	0.223	0.943		−0.114	0.114	0.988
653		−0.083	0.083	0.993		−0.112	0.112	0.999
683		−0.117	0.117	0.986		−0.154	0.154	0.998
713		−0.197	0.197	0.928		−0.217	0.217	0.994
Average			0.209				0.195	

SBG it rises from 0.249 (533 K) to 0.292 (563 K), drops to 0.112 (653 K) and peaks at 0.217 (713 K). This trend is similar to findings in literature [17]. The average value of n for AP and SBG is 0.209 and 0.195, respectively. Vuthaluru [39] performed a kinetic study on the pyrolytic behaviour of varied ratios of coal/biomass blend and for 0 to 100 ratios of coal/wood and coal/wheat straw, the values of n were 0.42 and 0.52 respectively. The values of n obtained in this study are slightly lower than those reported in literature. It is not an uncommon scenario as variation in the order of reaction of the various polymeric fractions of biomass has been noted by researchers [18, 38]. In fact, Meszaros et al. [40] in their investigation of hemicellulose pyrolysis assumed a second order reaction but observed significant distinction in the reaction order of the hemicellulose decomposition for diverse biomass materials. Moreover, the alkali metals in the ash content play a catalytic role in char formation, which in turn affects the chemical reactivity of the decomposition process [17]. This evidently influences the order of reaction as well. Thus, the complexity involved in the kinetics of lignocellulosic resources is clearly underscored with respect to biomass type and composition.

Conclusion

The HHV for AP (20.6 MJ kg^{-1}) was higher than for SBG (16.9 MJ kg^{-1}), while the ash content for SBG (7.54%) was higher than for AP (1.68%). FTIR spectroscopy also showed a clear distinction between AP and SBG in their levels of CC and lignin S/G ratios. The activation energy (E) varied significantly as conversion progresses yielding an average value of (DAEM; 227, Friedman's; 242 kJ mol^{-1}) for AP and (DAEM; 231, Friedman's; 231 kJ mol^{-1}) for SBG. The reaction order also varied with temperature and it was thus concluded that biomass decomposition follows a multi-step reaction mechanism.

Acknowledgments We acknowledge the financial support from the Lower Niger River Basin Development Authority sponsorship program.

References

1. van der Stelt, M.J.C., Gerhauser, H., Kiel, J.H.A., Ptasinski, K.J.: Biomass upgrading by torrefaction for the production of biofuels: a review. Biomass Bioenergy **35**, 3748–3762 (2011)
2. Mohammed, Y.S., Mustafa, M.W., Bashir, N., Mokhtar, A.S.: Renewable energy resources for distributed power generation in Nigeria: a review of the potential. Renew. Sustain. Energy Rev. **22**, 257–268 (2013)
3. Azeez, A.M., Meier, D., Odermatt, J., Willner, T.: Fast pyrolysis of African and European lignocellulosic biomasses using Py-GC/MS and fluidized bed reactor. Energy Fuels **24**, 2078–2085 (2010)
4. Vassilev, S.V., Baxter, D., Andersen, L.K., Vassileva, C.G.: An overview of the chemical composition of biomass. Fuel **89**, 913–933 (2010)
5. Lopez-Velaquez, M.A., Santes, V., Balmaseda, J., Torres-Garcia, E.: Pyrolysis of orange waste: a thermo-kinetic study. J. Anal. Appl. Pyrol. **99**, 170–177 (2013)
6. Soria, J.A., McDonald, A.G.: Liquefaction of softwoods and hardwoods in supercritical methanol: a novel approach to bio-oil production. In: Baskar, C., Baskar, S., Dhillon, R.S. (eds.) Biomass conversion: The interface of biotechnology, chemistry and materials science, pp. 421–433. Springer, Heidelberg (2012)
7. Huang, A., Zhou, Q., Liu, J., Fei, B., Sun, S.: Distinction of three wood species by Fourier transforms infrared spectroscopy and two-dimensional correlation IR spectroscopy. J. Mol. Struct. **883–884**, 160–166 (2008)
8. Osman, N., McDonald A.G., Laborie, M.-P.: Thermal compression of hybrid poplar wood: cellulose analysis. In: 5th European conference on wood modification 2010. Riga, Latvia (2010)
9. White, J.E., Catallo, W.J., Legendre, B.L.: Biomass pyrolysis kinetics: a comparative critical review with relevant agricultural residue case studies. J. Anal. Appl. Pyrol. **91**, 1–33 (2011)
10. Vand, V.: A theory of the irreversible electrical resistance changes of metallic films evaporated in vacuum. Proc. Phys. Soc. **A55**, 222–246 (1943)
11. Pitt, G.J.: The kinetics of the evolution of volatile products from coal. Fuel **41**, 267–274 (1962)
12. Solomon, P.R., Hamblen, D.G., Carangelo, R.M., Serio, M.A., Deshpande, G.V.: General model of coal devolatilization. Energy Fuels **2**, 405–422 (1988)
13. Várhegyi, G., Bobály, B., Jakab, E., Chen, H.: Thermogravimetric study of biomass pyrolysis kinetics: a distributed activation energy model with prediction tests. Energy Fuels **25**, 24–32 (2011)
14. Shen, D.K., Gu, S., Jin, B., Fang, M.X.: Thermal degradation mechanisms of wood under inert and oxidative environment using DAEM methods. Bioresour. Technol. **102**, 2047–2052 (2011)
15. Miura, K., Maki, T.: A simple method for estimating $f(E)$ and $k_0(E)$ in the distributed activation energy model. Energy Fuels **12**, 864–869 (1998)
16. Burnham, A.K., Oh, M.S., Crawford, R.W.: Pyrolysis of Argonne premium coals: activation energy distributions and related chemistry. Energy Fuels **3**, 42–55 (1989)
17. Gai, C., Dong, Y., Zhang, T.: The kinetic analysis of the pyrolysis of agricultural residue under non-isothermal conditions. Bioresour. Technol. **127**, 298–305 (2013)
18. Li, Z.Q., Zhao, W., Meng, B.H., Liu, C.L., Zhu, Q.Y., Zhao, G.B.: Kinetic study of corn straw pyrolysis: comparison of two different three-pseudocomponent models. Bioresour. Technol. **99**, 7616–7622 (2008)
19. Balogun, A.O., Lasode, O.A., McDonald, A.G.: Thermo-analytical and physico-chemical characterization of woody and non-woody biomass from an agro-ecological zone in Nigeria. BioResources **9**, 5099–5113 (2014)
20. Owen, N.L., Thomas, D.W.: Infrared studies of "hard" and "soft" woods. Appl. Spectrosc. **43**, 451–455 (1989)
21. Friedl, A., Padouvas, E., Rotter, H., Varmuza, K.: Prediction of heating values of biomass fuel from elemental composition. Anal. Chem. **554**, 191–198 (2005)
22. Cai, J., Liu, R.: New distributed activation energy model: numerical solution and application to pyrolysis kinetics of some types of biomass. Bioresour. Technol. **99**, 2795–2799 (2008)
23. Vyazovkin, S.: Modification of the integral isoconversional method to account for variation in the activation energy. J. Comput. Chem. **22**, 178–183 (2001)
24. Friedman, H.L.: Kinetics of thermal degradation of char-forming plastics from thermogravimetry. Application to a phenolic plastic. J. Polym. Sci. **6C**, 183–195 (1963)

25. Ruitenberg, G., Woldt, E., Petford-Long, A.K.: Comparing the Johnson-Mehl-Avrami-Kolmogorov equations for isothermal and linear heating conditions. Thermochem. Acta **378**, 97–105 (2001)
26. Volli, V., Singh, R.K.: Pyrolysis kinetics of de-oiled cakes by thermogravimetric analysis. J. Renew. Sustain. Energy **5**, 033130 (2013). doi:10.1063/1.4811794
27. Popescu, C.-M., Singurel, G., Popescu, M.-C., Vasile, C., Argyropoulos, D.S., Willför, S.: Vibrational spectroscopy and X-ray diffraction methods to establish the differences between hardwood and softwood. Carbohydr. Polym. **77**, 851–857 (2009)
28. Akerholm, M., Hinterstoisser, B., Salmen, L.: Characterization of the crystalline structure of cellulose using static and dynamic FT-IR spectroscopy. Carbohydr. Res. **339**, 569–578 (2004)
29. Santos, R.B., Lee, J.M., Jameel, H., Chang, H.M., Lucia, L.A.: Effects of hardwood structural and chemical characteristics on enzymatic hydrolysis for biofuel production. Bioresour. Technol. **110**, 232–238 (2012)
30. Chen, M., McClure, J.W.: Altered lignin composition in phenylalanine ammonia-lyase-inhibited radish seedlings: implications for seed-derived sinapoyl esters as lignin precursors. Phytochemistry **53**, 365–370 (2000)
31. Dai, J.: Conversion of woody biomass to polyhydroxybutyrate. Ph.D. Dissertation, University of Idaho, Moscow, ID, USA (2014)
32. Chen, D., Zheng, Y., Zhu, X.: In-depth investigation on the pyrolysis kinetics of raw biomass. Part I: kinetic analysis for the drying and devolatilization stages. Bioresour. Technol. **131**, 40–46 (2013)
33. Kim, S., Kim, J., Park, Y.-H., Park, Y.-K.: Pyrolysis kinetics and decomposition characteristics of pine trees. Bioresour. Technol. **101**, 9797–9802 (2010)
34. Naik, S., Goud, V.V., Rout, P.K., Jacobson, K., Dalai, A.K.: Characterisation of Canadian biomass for alternative renewable biofuel. Renew. Energ. **35**, 1624–1631 (2010)
35. Fisher, T., Hajaligol, M., Waymack, B., Kellogg, D.: Pyrolysis behaviour and kinetics of biomass derived materials. J. Anal. Appl. Pyrol. **62**, 331–349 (2002)
36. Balogun, A.O., Lasode, O.A., McDonald, A.G.: Devolatilisation kinetics and pyrolytic analyses of *Tectona grandis* (teak). Bioresour. Technol. **156**, 57–62 (2014)
37. Zhou, S., Garcia-Perez, M., Pecha, B., McDonald, A.G., Kersten, S., Westerhof, R.: Secondary vapor phase reactions of lignin derived oligomers obtained by the fast pyrolysis of pine wood. Energy Fuels **27**, 1428–1438 (2013)
38. Gronli, M., Antal, M.J., Varhegyi, G.: A round-robin study of cellulose pyrolysis kinetics by thermogravimetry. Ind. Eng. Chem. Resour. **38**, 2238–2244 (1999)
39. Vuthaluru, H.B.: Investigations into the pyrolytic behaviour of coal/biomass blends using thermogravimetric analysis. Bioresour. Technol. **92**, 187–195 (2004)
40. Meszaros, E., Varhegyi, G., Jakab, E.: Thermogravimetric and reaction kinetic analysis of biomass samples from an energy plantation. Energy Fuels **18**, 497–507 (2004)